Agricultural Water Management 327 (2026) 110284

Contents lists available at ScienceDirect

Agricultural Water Management

journal homepage: www.elsevier.com/locate/agwat

Integrating biophysical models and remote sensing to evaluate irrigation practices in four global hubs

Nikolas Galli [a,*], Francesco Capone [a], Jacopo Dari [b,c], Davide Danilo Chiarelli [a], Maria Cristina Rulli [a], Clément Abergel [d], Carla Saltalippi [b], Renato Morbidelli [b], Luca Brocca [c]

[a] Department of Civil and Environmental Engineering, Politecnico di Milano, Milano, Italy
[b] Department of Civil and Environmental Engineering, University of Perugia, Perugia, Italy
[c] CNR-IRPI, Perugia, Italy
[d] ECSAT, European Space Agency, Oxford, UK

ARTICLE INFO

Keywords:
Irrigation
Agriculture
Agrohydrological modelling
Remote sensing
Sustainable agriculture

ABSTRACT

Sustainable agricultural intensification through irrigation is necessary to address the challenges that climatic and demographic change pose to the global food system. This requires creating accurate regional-to-global knowledge bases of irrigation estimates, in a context where the availability of ground data is as valuable as infrequent. Large scale agro-hydrological models and irrigation estimates from earth observations are often associated with underrated yet significant uncertainties, but they also have complementary strengths and weaknesses. While already used in synergy for field-to-district scale applications, their synergistic use at larger scales remains unexplored. To fill this gap, we present a novel comparison of irrigation demand simulations from a spatially distributed agro-hydrological model and irrigation water use estimates from five satellite retrievals, over four global irrigation hubs. Despite describing different variables with independent tools running on independent data, the results show statistically significant linear correlations above 0.6 between biophysical simulations and satellite retrievals for three cases out of four. Moreover, space-time discrepancies pinpoint irrigation responses to hydroclimatic and anthropogenic drivers. Thus, a synergistic use of earth observation and large-scale agro-hydrological modelling, beyond mere data input, can improve our understanding of coupled human-natural dynamics in irrigation.

1. Introduction

Agricultural intensification through irrigation is often presented as one of the key assets to sustainably increase food production globally (Rosa et al., 2018). Indeed, despite covering 20% of the total cropland, irrigated lands provide 40% of the global crop production (Nagaraj et al., 2021). Irrigation boosts production by closing the yield gap, thus without requiring additional land. The key condition for the sustainability of irrigation is avoiding overdepletion of water resources that can cause water competitions in and downstream of the irrigation expansion areas (Chiarelli et al., 2022; Galli et al., 2023). To this add global challenges that intersect with the quest for irrigation expansion, putting additional constraints and creating additional risks. On one hand, climate change alters temperature and precipitation patterns, changing spatiotemporal gradients of both irrigation water demand and availability, and, as a consequence, the irrigation practices adopted by farmers. On the other hand, population growth and dietary transitions are far from uniform across regions, leading to spatially variable increases in agricultural and irrigation demand, which may further challenge the sustainability of irrigation practices (Mehta et al., 2024).

For instance, the Central Valley of California, one of the largest irrigated regions globally, faces growing challenges due to rising temperatures, reduced snowpacks, and altered precipitation patterns, which are making irrigation increasingly unsustainable (Lo and Famiglietti, 2013; Famiglietti et al., 2011). In India, the rice-wheat system has led to greater reliance on groundwater, resulting in depletion, with levels dropping by 1–3 m annually due to the limited capacity of water infrastructure and detrimental government subsidies for electricity used in water pumping (Devineni et al., 2022). Moreover, in the Mediterranean, recurrent droughts since the 1970s, combined with rising

* Corresponding author.
E-mail address: nikolas.galli@polimi.it (N. Galli).

https://doi.org/10.1016/j.agwat.2026.110284
Received 3 December 2025; Received in revised form 21 February 2026; Accepted 7 March 2026
Available online 15 March 2026

demands from socio-economic growth, are intensifying water scarcity (Iglesias et al., 2007). To manage these pressures, strategies such as improving water efficiency in agriculture, shifting to less water-intensive crops, and adopting effective water management practices are essential.

Many of these issues are addressed by modernizing and increasing the precision of irrigation systems, but also of irrigation models that typically support farmers and policymakers in their decisions (Dalezios et al., 2023). Yet, the global nature of the varying trends illustrated here, and of their impacts on agriculture, require increasing the accuracy of irrigation models also at higher scales. Global agro-hydrological models and satellite-driven irrigation models are two of the essential tools in this context. Agro-hydrological models combine hydrological processes with crop growth dynamics, quantifying irrigation demand with uncertainties that derive mainly from the integration of a variety of input factors, such as crop type, soil properties, climate variability, and soil moisture availability. Satellite-driven irrigation models, instead, provide estimates of irrigation by analyzing anomalies between actual evapotranspiration and soil moisture, both derived from earth observation (Dalezios et al., 2023). Both these classes of models can support, in different ways, the efficiency and adaptive capacity of irrigation. Yet, both have significant limitations that limit their efficacy and applicability in this purpose, which could at least partly be overcome by a conjunct utilization of the two.

While varying in their methodological approaches, ranging from process-based to data-driven, agro-hydrological models often already integrate data from earth observation, typically estimates of evapotranspiration, soil moisture, and vegetation indices (Eini et al., 2023, Dari et al., 2022). Established global agro-hydrological models, known for their contribution to the quantification of global irrigation demands, include AQUACROP (Kelly and Foster, 2021), the Global Crop Water Model (GCWM, Siebert and Döll, 2008), ACEA (Mialyk et al., 2024), and WATNEEDS (Chiarelli et al., 2020a). Most of these models are based on the FAO approach, that computes reference evapotranspiration from atmospheric conditions, potential crop evapotranspiration by integrating crop growth parameters and seasonality, and limits this potential evapotranspiration with available soil moisture obtained from solving the water balance in the active soil layer (Allen et al., 1998). This approach partitions crop water requirements into green water, i.e. evapotranspiration from precipitation-generated available soil moisture, and blue water (BW), as the demand for irrigation water to compensate for green water deficit with respect to total crop water requirement. Each model then modifies this approach to adapt it to its specific scope and goals. This, the uncertainty associated with the inputs, and other procedural differences make the outputs of these models diverge (Mialyk et al., 2024, Chiarelli et al., 2020a, Siebert and Döll, 2010), especially in areas with low data availability and accessibility. Another consequence of this approach is that most large scale agro-hydrological models are mainly focused on simulating biophysical water demand. When the focus is shifted towards simulating actual water withdrawals, it is often done so with rather constraining assumptions. Indeed, relying on hyperparametrized procedures with several arbitrary choices both in the assessment of water demand and in relating this to water withdrawals, large-scale agro-hydrological models provide estimates of irrigation withdrawal whose uncertainty is often overlooked (Puy et al., 2022).

Remote sensing irrigation estimates, on the other hand, provide representations of actual irrigation water use, but with strong assumptions on underlying physical processes. Earth Observations retrievals of land surface variables that can be a proxy for irrigation occurrence are potentially usable to derive irrigation water use (IWU) estimates. Approaches typically differ between those soil-moisture-based (e.g., Lawston et al., 2017; Brocca et al., 2018; Zappa et al., 2022), evapotranspiration-based (e.g., Brombacher et al., 2022; Kragh et al., 2023, Zipper et al., 2024), and those exploiting both soil moisture and evapotranspiration estimates. An alternative distinction, independent on the input variable leveraged, can be made between methods relying on the soil water balance (see, e.g., Jalilvand et al., 2019; Dari et al., 2022; 2025) and approaches exploiting the discrepancies between remotely sensed and modeled variables (Zaussinger et al., 2019; Koch et al., 2020; Kragh et al., 2024), under the assumption that the former track irrigation dynamics while the latter do not. Two well-established methodologies, one based on the soil water balance and one relying on satellite-modeling discrepancies, integrating EO soil moisture and evapotranspiration retrievals are the SM-Inversion and SM-Delta methods. Laluet et al. (2026) recently provided a systematic comparison of similarities and differences in the results from the two approaches on four irrigation hotspots worldwide: CONUS, Ebro basin (Spain), India, and Murray-Darling basin (Australia). To do this, the study was designed to share the same soil moisture inputs, namely ASCAT (Advanced SCATterometer), CCI (Climate Change Initiative) PASSIVE, CCI COMBINED, SMOS (Soil Moisture and Ocean Salinity), and SMAP (Soil Moisture Active Passive).

Dynamic satellite products can also compensate for limitations of agro-hydrological models arising from the use of static input data, especially in crop distribution and cropping calendars. On the other hand, satellite products at global scale typically have coarser resolutions than global agro-hydrological models, and are unable to differentiate among different land and crop covers within a single pixel, unlike agro-hydrological models (Zhang et al., 2022). Moreover, large uncertainties are still detected when comparing satellite estimates to ground measurements (Foster et al., 2020). Recent assimilation experiments of satellite driven products into physically based land surface models have shown promising results, even though still highly reliant on correct parametrization (Jalilvand et al., 2023). Thus, agro-hydrological models, providing dynamic and crop-specific accounting of irrigation demand, can support satellite products in understanding how their pixel-level estimate is the envelope of several different dynamic irrigation flows. Moreover, while irrigation estimates from remote sensing may provide more accurate depictions of actual irrigation dynamics, agro-hydrological models are more flexible to scenario implementations, including but not limited to climate change.

It thus emerges that biophysical irrigation demand modelling and satellite-driven irrigation water use estimates have complementary strengths and weaknesses. Therefore, combining these two products by leveraging their complementarity can drive significant improvements in understanding irrigation dynamics. While this is an already experimented procedure in small-scale studies, with fine-scale satellite observation and plot-to-district scale hydrological models, large-scale comparisons are widely unexplored.

Here we engage into such an analysis, comparing the results of a global agro-hydrological model and a suite of irrigation water use estimates from earth observation on four case studies representing important agricultural hubs in different continents. In particular, we rely on satellite estimates based on the soil moisture based inversion framework, which has proven particularly promising in providing accurate estimates at regional scale (Kragh et al., 2024), and on the spatially distributed, dynamic and crop-specific agro-hydrologcial model WATNEEDS (Chiarelli et al., 2020). We extract irrigation time series and compare the two types of products using error and correlation metrics (mainly root mean square error and Pearson correlation), identifying margins for mutual improvement in both methodologies. Moreover, we directly analyze seasonal and occasional fluctuations of these errors to investigate responses in irrigation to exogenous (climatic and anthropogenic) drivers. By doing this, we aim to provide a proof-of-concept of the value of analysing discrepancies between process-based and earth-observation based irrigation timeseries. While this analysis is just a comparison that does not attempt a substantial merging of the two techniques, it provides evidence that such a merging could improve our knowledge of mixed human-natural dynamics shaping irrigation in space and time, including for instance adaptation measures to specific hydroclimatic conditions, responses to hydroclimatic extremes, and the adoption of specific agricultural practices otherwise known at a predominantly local scale.

2. Methods

2.1. Case studies

The large-scale comparative analysis between biophysical irrigation demand and anthropogenic irrigation water use is performed on four global agricultural hubs, where irrigation plays a crucial role, as precipitation is not able to satisfy the whole atmospheric evapotranspirative demand (Table 1). The first case study focuses on the Continental United States (CONUS), which represents one of the most extensive and productive agricultural regions globally. Within this area, irrigated croplands account for approximately 14.5% of the total cultivated area. The region is largely characterized by extensive agriculture, dominated by cereal production such as maize, wheat, and soybeans, a significant portion of which is rainfed (FAO, 2024). Nevertheless, agriculture in CONUS is strongly dependent on irrigation, particularly in arid and semi-arid zones where water availability determines crop productivity. The main irrigation hubs are located in the California Central Valley, the Snake River Plains, the Great Plains, and the Mississippi floodplain, where irrigation infrastructure plays a crucial role in maintaining high yields. The analysis is restricted to grid cells in which at least 15% of the area was irrigated; nonetheless, this criterion still encompassed 99% of all irrigated areas within the region. The total annual agricultural water consumption for each case study is estimated from the agro-hydrological model WATNEEDS (Chiarelli et al., 2020b). For the CONUS case study it emerges that the annual agricultural water consumption is approximately 9.73×10^{10} m^3 , underscoring the substantial water demand associated with crop production in this region.

The second case study focuses on India, a country where irrigation plays a pivotal role in sustaining agricultural productivity. The main irrigation hubs are located within the Indo-Gangetic Plain, particularly in the Punjab–Haryana and Uttar Pradesh regions in the north, and in the West Bengal area in the east, near the border with Bangladesh. Another major irrigation hotspot is found in the Krishna–Godavari Delta, in southern India. Irrigation is essential for the cultivation of rice and wheat, which dominate the country's agricultural landscape (FAO, 2024). Within India, irrigated croplands account for approximately 44.4% of the total cultivated area, reflecting the heavy reliance of Indian agriculture on managed water resources. The country has developed an extensive network of canals and water conveyance systems, particularly throughout the Indo-Gangetic Plain, to support irrigation practices. Annual irrigation water consumption is extremely high, reaching about 3.21×10^{11} m^3 , underscoring the critical role of water management in maintaining food production and agricultural resilience across the region. The analysis considers 99% of all irrigated areas, achieved under the constraint of considering only cells with more than 15% irrigated area.

The third case study focuses on the Ebro River Basin, located in the eastern part of Spain. This study area is considerably smaller than the previous cases and concentrates on a single river basin characterized by a strong agricultural vocation. Approximately 24% of the total cultivated area within the basin is irrigated, mainly in the central section and the Ebro Delta. Irrigation supports a wide range of crops that would otherwise be constrained by the semi-arid climate typical of the region, particularly during the Summer months. Agricultural water consumption in the Ebro Basin is estimated at around 2800 million m^3 /y, which represents around 16% of the total irrigation water use in Spain.

The fourth case study focuses on the Murray–Darling Basin, located in the southeastern region of Australia. In this area, irrigated croplands account for only 11.4% of the total cultivated land, with an estimated annual irrigation water consumption of 8800 million m^3 /y. However, irrigation within the Murray–Darling Basin represents approximately 73% of the total irrigation water use in Australia, underscoring its dominant role in the country's agricultural water demand. Water scarcity severely limits the expansion of irrigated agriculture across most of Australia, making the Murray–Darling Basin an essential hub for agricultural production and national food security. This basin therefore, plays a critical role in balancing water management, crop productivity, and the sustainability of Australia's agricultural sector.

Table 1
Average rainfall and potential evapotranspiration over the four case studies. Data are averaged spatially over pixels with > 15% irrigated areas, and temporally over the 2003–2022 period, to maintain consistency with the analysis.

	CONUS	EBRO	INDIA	MURRAY-DARLING
Mean annual rainfall (mm/year)	654.4	452.4	1045.7	433
Mean annual PET (mm/year)	1231.9	1061.8	1475.6	1374.4

2.2. Blue water demand modelling

Blue water demand is modelled using the WATNEEDS spatially distributed, physically based, dynamic agro-hydrological model. WATNEEDS takes as input climatic variables, crop and soil parameters and performs crop- and location-specific soil water balances in the root zone, with a daily timestep. More specifically, it computes the following water balance equation for each crop *i* in pixel *j*:

$$\frac{\Delta S_{i,j}}{\Delta t} = P_{eff,j} - ET_{a,i,j} - D_{i,j} - R_{i,j} \quad (1)$$

Where:

- P_{eff} is effective rainfall, based on the assumption that 5% of precipitation is immediately directed to surface runoff. This hypothesis derives from Hoogeveen et al. (2015) and a sensitivity analysis to it has been conducted, for WATNEEDS, e.g. in (Galli et al., 2023).
- $ET_{a,i,j}$ is the actual evapotranspiration, corresponding to green water demand. This is obtained starting from the potential evapotranspiration:

$$ET_{i,j} = k_{c,i} \times ET_{0,j} \quad (2)$$

Where $ET_{0,j}$ is the reference evapotranspiration, obtained from the FAO-Penman-Monteith equation (Allen et al., 1998) and $k_{c,i}$ is the dynamic crop coefficient.

Potential evapotranspiration is limited by soil water availability through a stress coefficient k_s, which decreases linearly from 1 to 0 as the soil moisture decreases from the maximum allowable depletion, i.e. the soil moisture level below which crops enter water stress conditions, to the crop wilting point.

- $D_{i,j}$ is deep percolation below the root zone. The process is set on when soil moisture is higher than field capacity, and is modulated by soil moisture level and maximum infiltration rate (Chiarelli et al., 2020b).
- $R_{i,j}$ is runoff.

Blue water (irrigation) requirements are then obtained as the difference between stressed (actual) and unstressed (potential) evapotranspiration.

$$BW_{i,j} = ET_{i,j} - ET_{a,i,j} \quad (3)$$

Daily results are cumulated monthly, and pixel-level BW estimates are obtained through a weighted sum of crop-specific requirements, with the weights being crop-specific irrigated areas $A_{i,j}$:

$$BW_j = \frac{\sum_i BW_{i,j} \times A_{i,j}}{\sum_i A_{i,j}} \tag{4}$$

WATNEEDS is run for the period 2003–2022, following its most commonly used settings, reported in (Chiarelli et al., 2020b), for what concerns meteoclimatic, soil and crop inputs, as well as resolution. This means that the model is run at 5 arc-minutes resolution (ca. 10 km at the equator) and then the results are resampled and aggregated to match the resolution of the remote-sensing derived irrigation estimates.

2.3. Remote-sensing derived irrigation estimates

Remote-sensing based irrigation water use (IWU) estimates are obtained through the SM-Inversion algorithm (Dari et al., 2023; 2024), originally born to retrieve rainfall rates by inverting the soil moisture signal (Brocca et al., 2014). The method was later adapted to estimate IWU (Brocca et al., 2018; Dari et al., 2020). In fact, over agricultural areas the total amount of water entering the soil (the actual algorithm output) is determined by the sum of rainfall and irrigation rates; hence, by removing rainfall rates from the algorithm output, it is possible to estimate the amount of water applied for irrigation. For each pixel, the soil water balance is expressed as follows:

$$nZ\frac{\Delta S}{\Delta t} = IWU(t) + P(t) - G(t) - R(t) - ET(t) \tag{5}$$

In which n [-] is the soil porosity, Z [mm] is the soil layer depth, $\Delta S/\Delta t$ [-] is the variation of relative soil moisture (i.e., between 0 and 1) in time, t [day], $IWU(t)$ [mm/day] is the applied irrigation rate, $P(t)$ [mm/day] indicates the rainfall rate, $G(t)$ [mm/day] represents the drainage rate, intended as the sum of deep percolation and subsurface runoff, $R(t)$ [mm/day] is the surface runoff, and $ET(t)$ [mm/day] is the actual evapotranspiration rate. Eq. (5) can be also written as:

$$Win\ (t) = Z^*\frac{\Delta S}{\Delta t} + G(t) + R(t) + ET(t) \tag{6}$$

In which $Win(t)$ [mm/day] represents the total amount of water entering the soil, namely $Win(t) = IWU(t) + P(t)$; $Z^* = nZ$ [mm] is the amount of water that can be stored into the soil layer. Based on previous studies, the $R(t)$ term is neglected (Brocca et al., 2015), while the drainage term is expressed as a function of soil moisture:

$$G(t) = aS(t)^b \tag{7}$$

a [mm] and b [-] are parameters linked to the infiltration capacity of the soil. The $ET(t)$ term is computed by adopting a water-limit approach, i.e., by limiting the potential evapotranspiration rate, $PET(t)$, through the available water content:

$$ET(t) = F \times S(t) \times PET(t) \tag{8}$$

with F [-] indicating a scaling factor (Dari et al., 2023; 2024). Eq. (2) can then be written as follows:

$$Win(t) = Z^*\frac{\Delta S}{\Delta t} + aS(t)^b + F \times S(t) \times PET(t) \tag{9}$$

Z^*, a, b, and F are algorithm parameters that need to be calibrated. In line with the recent implementation by Dari et al. (2024), the calibration is carried out by using rainfall as a target, i.e., by optimising the method performances in properly reproducing rainfall amounts during the non-irrigation periods, in which the left term on Eq. (5) is supposed to be determined by rainfall only. The calibrated algorithm parameters are then used to estimate IWU during the irrigation season. In such periods, both rainfall and irrigation rates potentially contribute in determining the left term of Eq. (5), so irrigation estimates can be obtained as: $IWU(t) = Win(t) - P(t)$. If weekly estimates of IWU result lower than 20% of weekly rainfall, they are discarded as likely due to propagation of random errors. Finally, eventual negative IWU rates are set equal to zero (Dari et al., 2023). To delineate irrigation and rainfed seasons, the calendar provided by Portmann et al. (2008) plus ancillary information are used. IWU estimates are produced during irrigation seasons indicated in Table 2 and over areas equipped for irrigation. The latter information is derived from the latest version of the global map of areas equipped for irrigation by Mehta et al. (2022). In detail, only pixels more than 5% of area equipped for irrigation are considered (Laluet et al., 2025; Dari et al., 2025).

IWU estimates are produced by leveraging five different soil moisture products (Table 3): Advanced SCATterometer (ASCAT), Level 2 Soil Moisture Ocean Salinity (SMOS L2), Level 2 Soil Moisture Active Passive (SMAP L2), and Climate Change Initiative (CCI) Combined (CCI COMBINED) and Passive (CCI PASSIVE) data sets. The Global Land Evaporation Amsterdam Model (GLEAM) v3.7b (Martens et al., 2017) is used as a source for potential evapotranspiration data, while the ERA5 (European ReAnalysis v5) (Hersbach et al., 2020) lowest model level forecasts are considered for rainfall rates. Simulations leveraging different soil moisture products cover different periods because of the temporal coverage of each sensor. However, for all the simulations half of the total time series has been used for the calibration of the algorithm parameters; the irrigation estimates cover the whole period of data availability. Note that the overlapping of calibration and validation periods during the first half of the time series does not affect the reliability of the results in terms of irrigation estimates because of the complementarity between rainfed and irrigation seasons.The IWU products developed through the SM-Inversion method are available at https://zenodo.org/records/14988198 (Laluet et al., 2025b). Since the input data sets are characterized by different spatial resolutions, they have all been resampled to a common 0.25° regular grid prior to the analysis (Table 3).

2.4. BW vs. IWU intercomparison

WATNEEDS outputs are resampled to the 0.25° regular grid adopted for the satellite-based IWU estimates to ensure spatial consistency, and the two sets of products are combined into a multivariable dataset. To exclude areas where the signal of satellite data is too noisy, pixels with less than 15% of area equipped for irrigation are removed. The area equipped for irrigation is based on MIRCA-OS data (Kebede et al., 2024), the same used as crop cover input by WATNEEDS.

To understand how WATNEEDS is positioned with respect to satellite products and their reciprocal differences in each case study, we extract case-study timelines of mean and standard deviation of irrigation. This allows us to visualize temporal patterns of all series at once, highlighting time or event-specific discrepancies in each case study. On the other hand, it only shows overall discrepancies between time series, virtually considering each case study as a single observation point, with internal spatial gradients being treated as a source of uncertainty. Therefore, as a complement, we also create an average monthly spatialized time series of each dataset, where each pixel reports, for each month, the average value across the years for that month and pixel. We compute the difference of this time series between WATNEEDS and each of the satellite models and analyze the distribution of these discrepancies over each of the four case studies. Finally, we calculate pixel-level linear correlations between WATNEEDS and each satellite-based product, for the whole time series. For long term differences and pixel-level linear correlations, off-season months where satellite-based products are set to zero a priori

Table 2
Irrigation seasons considered in the implementation of the SM-Inversion algorithm over the case studies.

	Adopted irrigation season
CONUS	September-April
Ebro basin	May-September
India	November-June: Rabi (November-March) and Zaid (April-June)
Murray-Darlin basin	April-October

Table 3
Products, versions, and spatial and temporal resolution of satellite products utilized.

Short name	version	Spatial/temporal sampling
CCI PASSIVE	v08.1 - TU Wien	0.25°/daily
CCI COMBINED	v08.1 - TU Wien	0.25°/daily
SMOS	SMOS L2 SM v700	35–50 km/3 days
SMAP	SMAP L2 v8	36 km/3 days
ASCAT	Climate Data Record v7 12.5 km sampling	12.5 km/daily

are excluded from the sample.

3. Results

Fig. 1 reports spatially averaged time series for each case study, showing how irrigation evolves seasonally and over the years in the four case studies, according to physically based modelling of irrigation demand and Earth-Observation driven estimates of IWU. What emerges overall is that WATNEEDS BW time series are comparable with IWU from satellite products. In particular, the shaded envelope representing ±1 standard deviation from WATNEEDS overlaps with at least one of the shaded envelopes of satellite retrievals during the whole period for all case studies. Overall error metrics between WATNEEDS and satellite retrievals depend largely on the satellite-based product and the case study. Table 4 reports root mean square errors and linear correlations of WATNEEDS with respect to satellite retrievals for the time series reported in Fig. 1. India is the worst performing case study with both the highest RMSE (23.4 mm, for CCI-PASSIVE) and the only close-to-zero correlations (for SMAP, SMOS, and CCI PASSIVE). Other case studies present satisfactory agreements, like the linear correlations above 0.8

Table 4
Root mean square errors and linear correlation coefficients between WATNEEDS and satellite retrievals, for the average time series over each case study. Correlations marked by '***' have a p-value lower than 0.001. Unmarked correlations have a p-value higher than 0.1.

RMSE (mm/month)	ASCAT	SMAP	SMOS	CCI-COMBINED	CCI-PASSIVE
CONUS	6.8	7.0	9.4	8.1	7.3
Ebro Basin	7.4	7.5	7.5	9.1	12.2
India	19.9	22.9	20.5	13.7	23.4
Murray-Darling basin	11.4	7.8	7.8	7.7	7.4

Pearson correlation	ASCAT	SMAP	SMOS	CCI-COMBINED	CCI-PASSIVE
CONUS	0.87***	0.84***	0.82***	0.81***	0.85***
Ebro Basin	0.64***	0.65***	0.72***	0.71***	0.75***
India	0.32***	0.07	-0.07	0.32***	0.04
Murray-Darling basin	0.65***	0.69***	0.71***	0.68***	0.77***

for all products in the CONUS case study. Overall, physically based modelling of BW and satellite estimates of IWU tend to agree on the main seasonal patterns and on the magnitude of irrigation intensity in each case study, despite representing different variables (demand vs. use) estimated with independent data and approaches. Discrepancies, instead, arise especially for specific case studies and periods. The main one is visible for India, where WATNEEDS correctly describes the irrigation season occurring between April and June but consistently underestimates the one occurring between November and February-March, leading also to the negative correlation reported in Table 4. This is mainly linked to the presence of multiple rice-growing seasons (Chiarelli et al., 2020b), and to the fact that WATNEEDS does not capture one of the rice production cycles. Between November and June, satellite estimates clearly capture irrigation signals associated with the

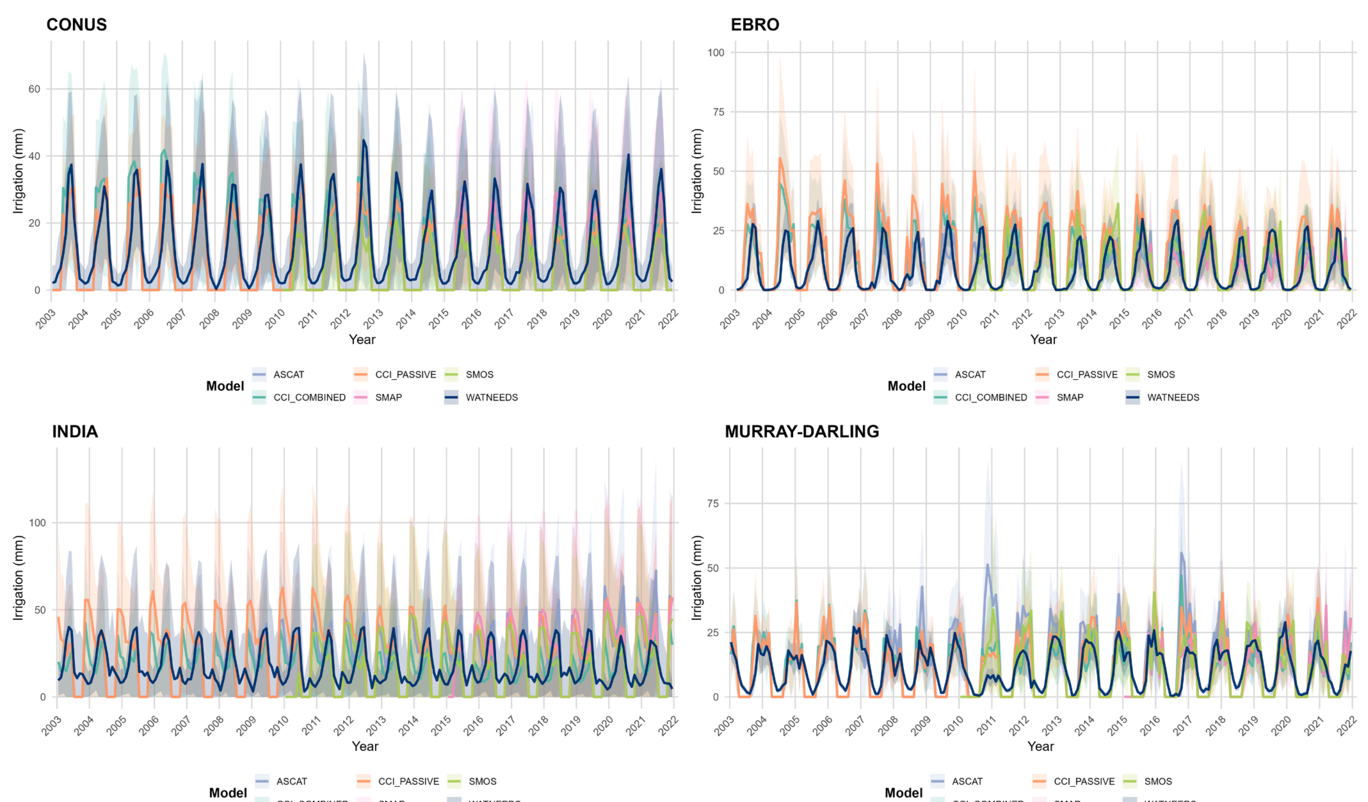

Fig. 1. Time series of BW by WATNEEDS and IWU by satellite products. Lines represent averages over the case studies, while shaded bands represent ±1 standard deviation from the average.

Rabi and Zaid rice cycles, whereas WATNEEDS only represents the dominant Kharif crop. As a result, early-season irrigation peaks are systematically underestimated by the model. Kharif rice, planted in June–July and harvested in September–October, accounts for around 70% of the national rice production and is largely rainfed, thus requiring limited irrigation (U.S. Department of Agriculture, 2025). By contrast, Rabi rice, grown in the Winter–Spring season (November–April), represents a smaller share of production (≈10–15%) but relies almost entirely on artificial irrigation, making it highly water-intensive (U.S. Department of Agriculture, 2025). The discrepancy this practice generates is even more visible in Fig. 2, reporting distributions over the case study of long-term average differences between satellite-based products and WATNEEDS. It is evident that, while for April to June the difference is quite evenly distributed around zero for all products, the confidence bars present an asymmetrical shift towards positive values between November and February. Since both WATNEEDS and the SM-inversion approach are based on pre-imposed irrigation seasons, this discrepancy highlights a difference in assumptions of the two approaches, and shows how their conjunct use can help identifying and overcoming such limitations.

In the Murray–Darling Basin case study, WATNEEDS fails to reproduce the pronounced peaks visible in the satellite-derived products along the long-term time series. This divergence is particularly evident in 2010–2011 and again in 2017, when satellite IWU estimates (e.g. those from ASCAT and SMOS products) detect strong maxima, whereas WATNEEDS shows much lower values. The most plausible explanation is that WATNEEDS, being a biophysical model of irrigation demand, does not account for large-scale flood events that periodically affect the Basin. During major floods, the demand for irrigation water is drastically reduced, while the presence of inundated areas increases evaporation and surface moisture, which in turn enhances the signal captured by satellite retrievals of actual water use. Note that such a circumstance can also be translated into potential irrigation overestimates. This mechanism was already documented for the 2010–2011 flood, one of the most extensive in recent history (Whitworth et al., 2012). More recently, another large-scale flood event occurred in 2016–2017, also reported in the literature as a driver of significant increases in wetland inundation and evapotranspiration across the Basin (Chen et al., 2021). The mismatch between WATNEEDS and satellite estimates can thus be largely attributed to the occurrence of these extreme hydrological events, which are not represented in WATNEEDS but can be tracked by satellite-based observations.

WATNEEDS shows a peak in BW higher than IWU peaks of satellite-based use products in 2012 in the CONUS case study. Situations where irrigation demand is much higher than actual irrigation are typical for droughts, and indeed the U.S. Drought Monitor reports a historic peak in cumulative percentage of drought areas for the Summer of 2012 (United States Drought Monitor, 2022).

In the Ebro Basin, differences between WATNEEDS and satellite products are most evident at the onset of the irrigation season. Satellite-based estimates of actual IWU show a sharp increase in April, while WATNEEDS simulates a much more gradual rise in BW. This discrepancy may reflect Spring irrigation practices diffused in some parts of the Ebro basin and thus captured by satellite sensors including high-resolution retrievals (Zappa et al., 2024, Dari et al., 2023), whereas WATNEEDS, as a biophysical model, does not identify a demand for irrigation. As a result, WATNEEDS underestimates the early-season peak in irrigation water use observed in the satellite products (Chiarelli et al., 2020a; Maltby, 2006).

Seasonal discrepancies, not related to specific events but occurring regularly during certain times of the year, are more easily identifiable from Fig. 2. For instance, it appears that differences between satellite products and WATNEEDS tend to present a slight positive shift at the beginning of irrigation periods, then gradually move towards negative shifts in the middle of the period, and back to differences more symmetrically distributed around zero at the end of the irrigation season.

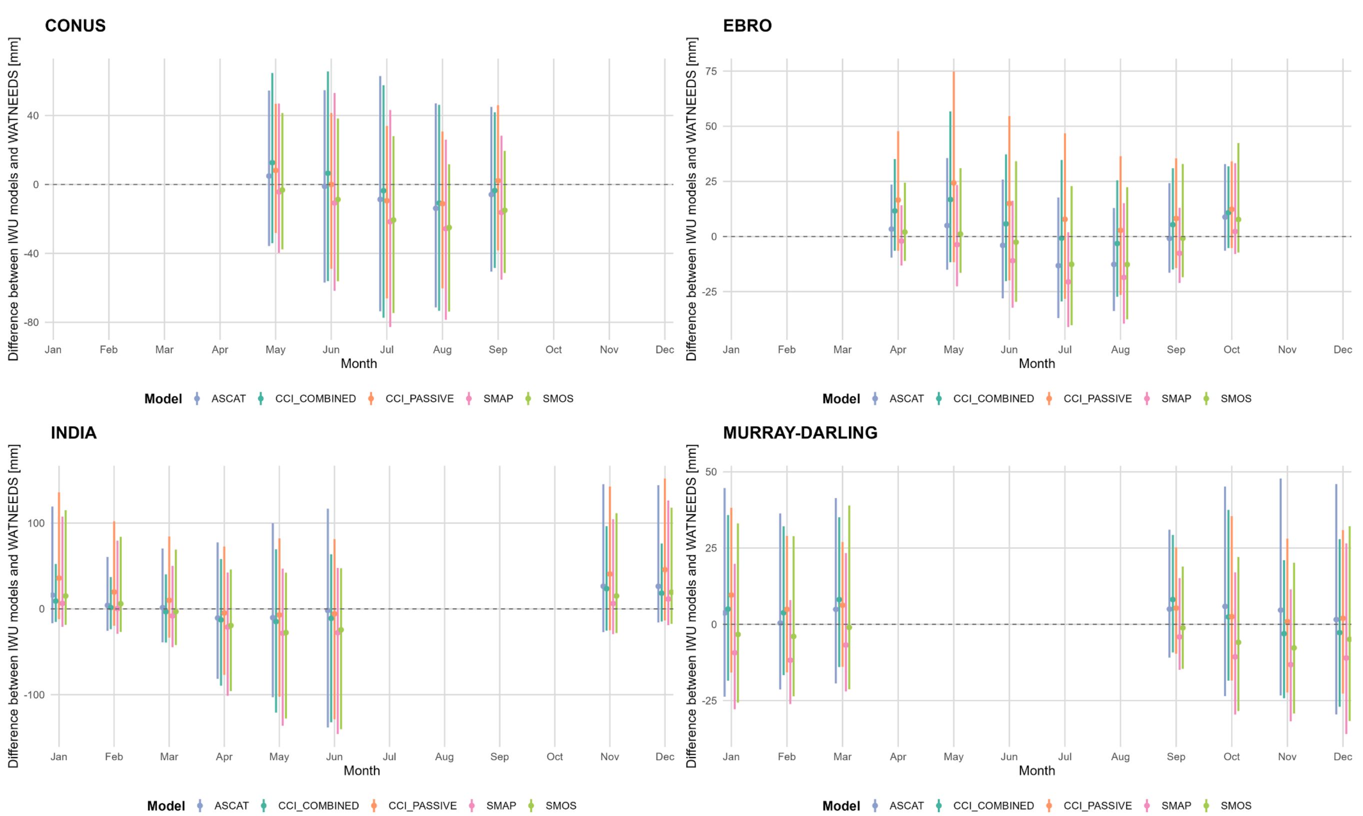

Fig. 2. Long-term average time series of differences between WATNEEDS BW and satellite IWU estimates. Points represent averages over the case study, while error bars span from 0.05 to 0.95 quantiles of differences.

This happens regardless of the case study and of the time of the year during which the irrigation season occurs. As for previously analyzed differences, it is at least partially explainable as a discrepancy between biophysical irrigation demand and actual irrigation provision. The irrigation demand closely follows the evolution of the local climate, increasing during local Summer, when temperatures increase and precipitation rates decrease. Irrigation application, on the other hand, likely follows less regular patterns, conditioned by water management practices. This is also visible in Fig. 1, especially for the Ebro and Murray-Darling case studies, where the periodicity of WATNEEDS is more sinusoidal, while satellite estimates have more noisy oscillations during irrigation seasons. Connected to this, WATNEEDS computes a demand for irrigation water also outside of what satellite products consider as irrigation season. Thus, there might be an irrigation application at the beginning of the season, observed by satellite products, which WATNEEDS underestimates because it has already accounted for irrigation demands arising before season start.

These results help understand how physical modelling and Earth Observation provide different, sometimes complementary, interpretations of irrigation dynamics over different spatial scales, allowing to investigate responses to specific events and adaptations to seasonal patterns. Correlation maps reported in Figs. 3–6 add to this understanding providing information on local spatial gradients of agreement between physical modelling and earth observations. Linear correlation appears to be site specific, with marked spatial gradients within case studies. Overall, the Ebro basin presents better performances, with consistent moderate positive correlations across the study area, reaching an average cross-basin correlation of 0.38 with CCI_PASSIVE. Specific regions in CONUS and India reach correlations above 0.80. Despite this, some combinations of regions and retrieval for CONUS exhibit negative correlations, for instance the California Valley for the CCI_COMBINED retrieval. In India, instead, this behaviour regards extensive regions for most products. The Murray-Darling basin also has a varied behavior, with most areas presenting moderate positive correlations between WATNEEDS and at least one satellite retrieval, but also many areas for which negative correlations are observed. The general indication that emerges is an agreement increasing with the extent of irrigated areas. WATNEEDS is expected to be rather insensitive to this parameter, because it performs the vertical soil water balance for each crop in each pixel separately, and then creates a combined result weighting the single outputs by the irrigated areas of the crops. For satellite products, instead, smaller irrigated areas translate into a higher difficulty in properly solving mixed landscapes and disentangling the irrigation signal within the pixel, especially in case of coarse resolution retrievals as those considered in this study. In fact, the matching between the spatial resolution of satellite retrievals and the nominal extent of irrigated areas is a crucial issue to effectively monitor irrigation dynamics from space (Zappa et al., 2022; Dari et al., 2025). Thus, uncertainties inversely proportional to irrigated areas are less pronounced in WATNEEDS than in satellite products, and, for WATNEEDS, rather due to uncertainties in the input data on irrigated croplands than to the approach itself. Another interesting observation is that different satellite products perform differently across areas within the same case study. This is particularly evident in the CONUS case study. Three main irrigation hubs can be identified based on the map of irrigated areas, from West to East: the California Valley, the Snake River Plains, the Great Plains, and the Mississippi Floodplain. While the SMOS-based product has an agreement with WATNEEDS higher than any other product for the California Valley and the Snake River Plains, for the other two regions the highest agreement can be found for CCI products.

4. Discussion

Our results show that the conjunct and comparative analysis of BW simulated by biophysical modelling and IWU estimated from Earth Observations, even performed with straightforward approaches, can provide interesting insights not only into the limitations to the representativity of both methodologies, but also on human-water interactions and feedbacks characterizing irrigation use dynamics. This has been widely explored at small scales, especially with the aim of providing irrigation monitoring tools and informing local sustainable water management (Toureiro et al., 2017, Bwambale et al., 2022, Tolomio and Casa, 2020). Instead, moving towards the integration of irrigation water use estimates from space and global hydrological modelling is still an emerging research trajectory, potentially enabling novel considerations, techniques and instruments for regional-to-global water sustainability strategies. Our results are encouraging in regard to this direction, given the overall positive correlation found between IWU and BW, especially considering that the two variables have different degrees of dependency on different climatological variables (IWU on satellite-observed soil moisture, BW on PET and precipitation through crop-specific water budget and stress threshold mechanisms). Thus, rather than a spurious correlation with a common climatology, the agreement between IWU and BW suggests that, as could be expected, water applied to fields overall follows the trend of water demanded by crops, except for situations (e.g., floods, droughts, specific irrigation practices) which can be identified and characterized by looking at where and how IWU and BW diverge.

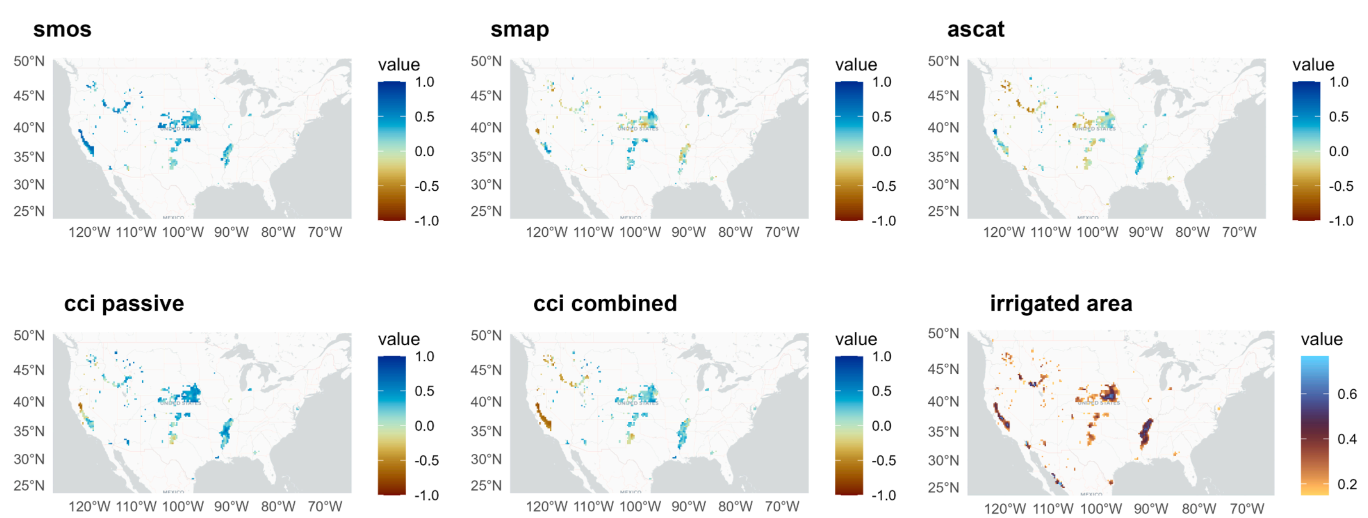

Fig. 3. Map of pixel-specific linear correlations for CONUS, between WATNEEDS BW and IWU from satellite retrievals. The bottom right map, instead, represents the pixel-specific irrigated fraction.

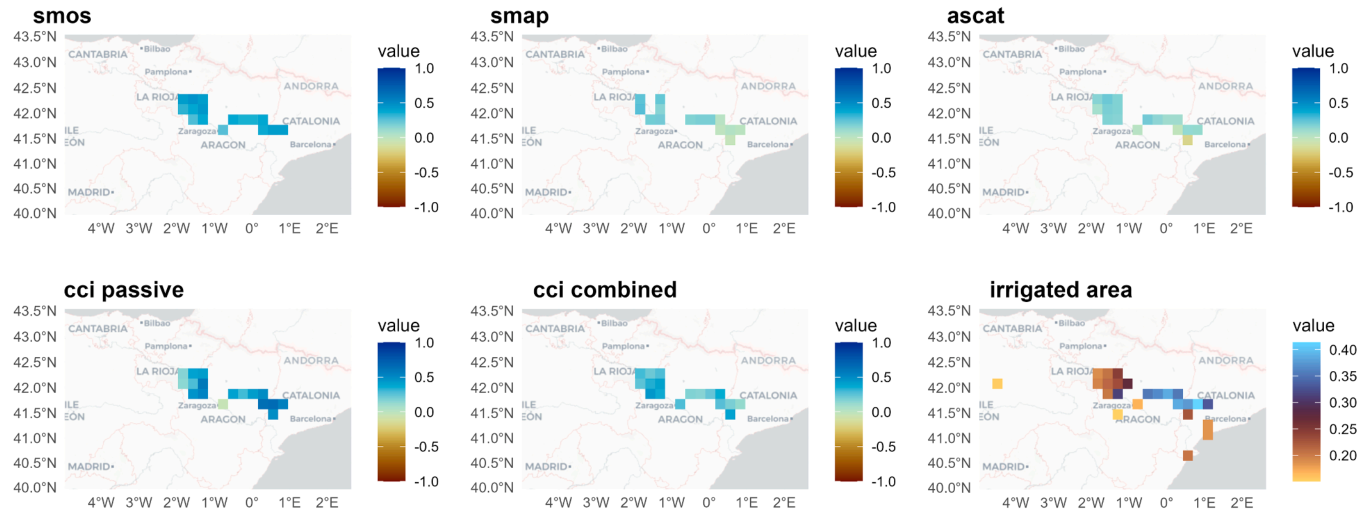

Fig. 4. Map of pixel-specific linear correlations for the Ebro basin, between WATNEEDS BW and IWU from satellite retrievals. The bottom right map, instead, represents the pixel-specific irrigated fraction.

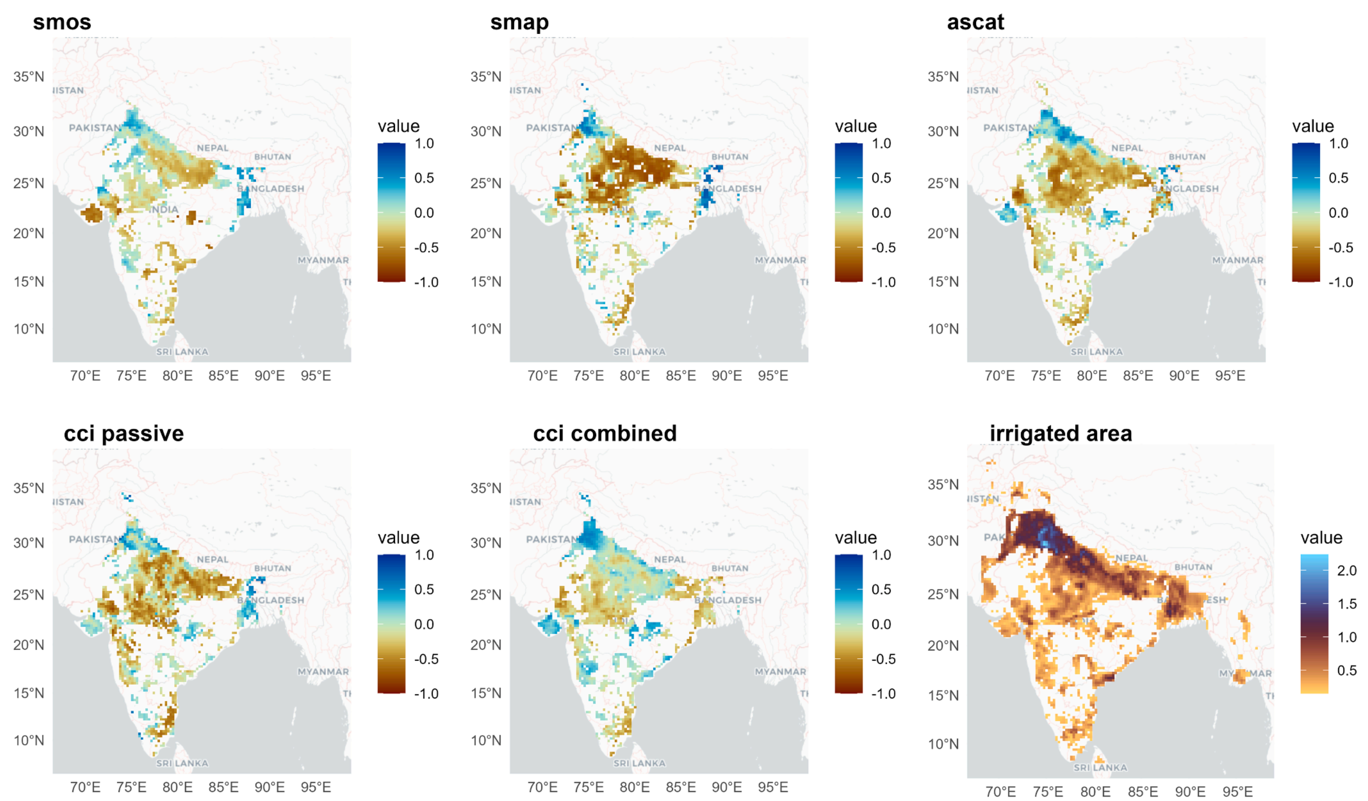

Fig. 5. Map of pixel-specific linear correlations for India, between WATNEEDS BW and IWU from satellite retrievals. The bottom right map, instead, represents the pixel-specific irrigated fraction.

In fact, comparing BW with IWU highlights how water use has responded to both acute and chronic exogenous drivers, including droughts, floods, and seasonal fluctuations in water availability. It also highlights similarities and differences in these responses between different contexts across the world. Therefore, there is margin for innovation in the conjunct use of these instruments, to inform large-scale studies on agricultural practices and their adaptation to climate change, extreme events, and other anthropogenic changes. Yet, this innovation potential requires research to overcome current limitations in both methodologies and to refine the techniques by which they are compared and integrated.

For instance, it emerges from our analysis that different satellite products have different levels of agreement with WATNEEDS in different areas, periods, and seasons. This means that using satellite-driven estimates of irrigation water use to improve agro-hydrological modelling requires methodologies to identify, for each agro-hydrological model, and possibly for each application, the best ensemble of satellite products, rather than using a single product. On the other hand, we identify common discrepancy patterns between WATNEEDS and all satellite-based products, especially when these derive from exogenous acute or seasonal factors, mostly connected to the fact that WATNEEDS models irrigation demand while satellite products

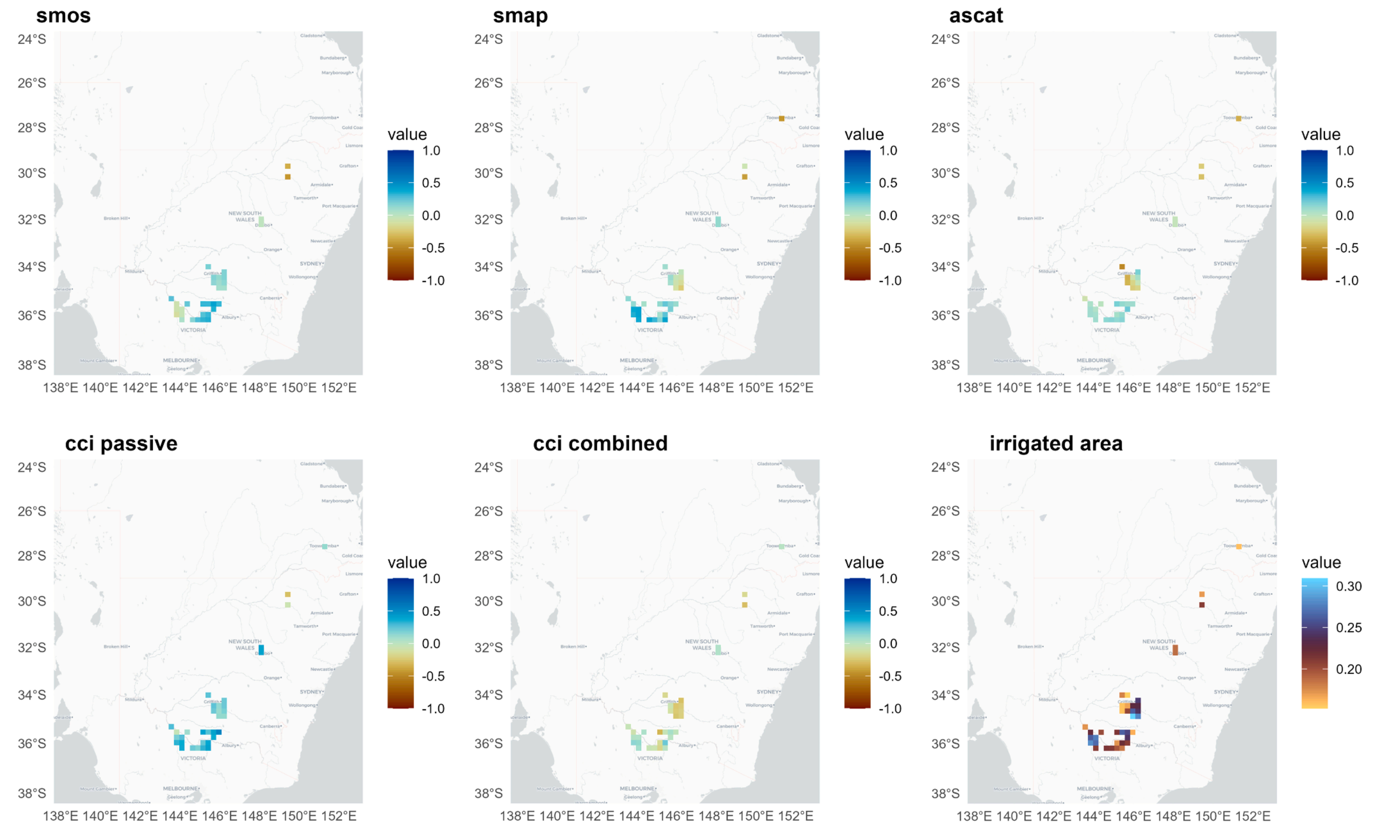

Fig. 6. Map of pixel-specific linear correlations for the Murray-Darling basin, between WATNEEDS BW and IWU from satellite retrievals. The bottom right map, instead, represents the pixel-specific irrigated fraction.

estimate irrigation water use. Clearly, both tools have their own sources of uncertainty, which have been detailed in previous validation efforts: the SM-inversion method has been recently validated against ground observations (Laluet et al., 2026), and WATNEEDS outputs have been validated against estimates from widely renowned modeling platforms and against MODIS estimates (Chiarelli et al., 2020). Disentangling uncertainties peculiar to one or the other method from those deriving from exogenous factors is therefore a necessary future development to correctly identify pathways of improvement for both techniques, as well as for refining our understanding of the feedbacks between irrigation demand and irrigation water use. This could be done e.g. developing a process-based algorithm to estimate IWU based on BW, using IWU from satellite retrievals as a calibration benchmark. Such a further integration of satellite estimates into biophysical modelling would both allow better separation of model error from actual differences between water demand and water use, and potentially also better interpretation of these discrepancies through explainable parameters used to force the process-based computation of IWU.

Another relevant aspect related to the agreement between WATNEEDS and satellite products is that this tends to increase when irrigated areas increase. This required us to limit the analyzed sample to areas having at least a 15% irrigated coverage, thus significantly reducing the size of the sample, especially for India, an already data-scarce region. Future research could leverage what currently is a source of uncertainty, for instance by obtaining information on biophysical processes from areas of high agreement, which could then be used to reduce the noise in satellite signals in other areas.

Besides validation efforts to characterize and limit the uncertainty associated with the SM-inversion approach itself, understanding how intrinsic uncertainty of input data propagates into output estimates also constitutes a key future development not only for satellite retrievals but also for agro-hydrological modelling. The constraint here is that in-depth characterizations of the uncertainty of input data, necessary to correctly analyze its propagation, is not always explicitly available.

A source of uncertainty which instead derives specifically from biophysical modelling is that WATNEEDS uses static information on croplands and, more importantly, irrigated areas. Therefore, it is not possible for WATNEEDS to observe trends of expansion, or possibly of abandonment, of irrigated lands with currently used inputs, trends which would instead be captured by satellite products. This does not seem to be the case in the currently investigated application, as no significant increasing/decreasing trends are detected in irrigation estimates, neither in WATNEEDS nor in the satellite products. Yet, it might have contributed to inaccuracies in the representation of crop-specific and irrigation seasonalities. Indeed, common global cropping calendars are spatially distributed but static, meaning that they overlook key agricultural adaptation practices such as advances and delays in crop planting and harvesting. This limitation is therefore difficult to overcome: common ways to embed dynamic cropping calendars into agro-hydrological modelling, such as growing degree days functions, typically relate more closely to phenological and biophysical properties of the crop, rather than anthropogenic decisions based on empirical practices. Analogously, a necessary scoping limitation of this study is performing the analysis over recent historical data. Climate change projections of biophysical blue water demand are becoming increasingly feasible and reliable thanks to progress in global and regional circulation models, but uncertainties remain regarding crop-specific future land use change scenarios, as well as the impacts on phenologic cycles and cropping calendars, and on the other hand, climate projections of soil moisture would be modelled and not observed data, and thus not suited for SM-based inversion. Recent studies show that climate change has already exacerbated the pressure of irrigation on water resources in the past decades (Yao et al., 2025), and that future irrigation expansion, more than climate change, will drive an estimated 70% increase in blue water consumption by 2090, even though this irrigation expansion itself can be connected to a climate-change driven increase in irrigation dependency (Huang et al., 2019).

Finally, a main source of uncertainty deriving from both agro-hydrological modelling and Earth Observation is that both tools are applied in their most commonly used specifications. We do this specifically to assess the current state of agreement and to perform an initial analysis. One of the first steps towards a more in-depth harmonization of the two approaches is to harmonize the data they rely on.

In summary, disentangling discrepancies between hydrological modelling and satellite observation of irrigation by separating inherent uncertainties from conceptual differences, can transform the conjunct use of these two methods into a powerful instrument to understand commonly employed agricultural practices across scales and contexts, and how these practices are tuned to respond to different exogenous drivers. For instance, it could help better quantify the difference between the biophysical irrigation demand of rice and the water actually applied, especially to paddy rice fields, potentially overcoming key limitations of agro-hydrological modelling, but also deepening our knowledge on how these fields react to drought, on one hand, and contribute to drought mitigation, on the other hand (Galli et al., 2025). More in general, this study, by providing an initial large-scale comparative assessment of biophysical irrigation demand modelling and satellite-driven irrigation water use estimates, and by highlighting the limitations of such an assessment, paves the way for the development of more structured and refined analytical techniques, moving towards a tighter integration of process-based modelling and earth observation, into a new set of instruments for investigating water use in agriculture at regional-to-global scale.

5. Conclusion

Irrigation represents a key component of both agricultural productivity and water resource management, yet its quantification across large spatial scales remains challenging. Physically-based models and remote-sensing estimates offer complementary perspectives on irrigation dynamics, however they may occasionally diverge due to their differing conceptual and data frameworks.

This study serves as a proof-of-concept evaluation of the discrepancies and synergies between irrigation demand modelled by WATNEEDS and SM-inversion irrigation water use, highlighting how their integration can advance our understanding of irrigation processes, while also supporting the mutual improvement of both modelling and satellite-based approaches. WATNEEDS and remote-sensing products show consistent seasonal and spatial patterns, confirming the overall validity of the approach, with discrepancies mainly reflecting differences between biophysical irrigation demand and actual irrigation provision. Correlations vary across regions and satellite products, being higher in areas with greater irrigated extent and lower in fragmented regions. Our results show that combining the two approaches has the potential to enable a more comprehensive understanding of irrigation dynamics, bridging the gap between biophysical water demand and human water use. A main limitation is the use of static information on croplands and irrigated areas, which prevents capturing temporal changes and adaptive shifts in cropping calendars, a limitation which could also be at least partially addressed with integration of biophysical process modelling and earth observation. Future research should focus on harmonizing model inputs and satellite datasets to build integrated frameworks for irrigation monitoring and assessment. Overall, this study represents a first step towards integrating physically-based models and remote-sensing estimates into comprehensive tools for assessing irrigation and agricultural water use.

CRediT authorship contribution statement

Nikolas Galli: Writing – original draft, Visualization, Methodology, Investigation, Formal analysis, Conceptualization. **Francesco Capone:** Writing – original draft, Visualization, Methodology, Investigation, Formal analysis. **Jacopo Dari:** Writing – original draft, Methodology, Investigation, Formal analysis, Conceptualization. **Davide Danilo Chiarelli:** Writing – original draft, Methodology, Conceptualization. **Maria Cristina Rulli:** Writing – review & editing, Supervision, Methodology, Investigation, Conceptualization. **Clement Abergel:** Writing – review & editing, Supervision, Project administration, Conceptualization. **Carla Saltalippi:** Methodology, Formal analysis, Conceptualization. **Renato Morbidelli:** Methodology, Conceptualization. **Luca Brocca:** Writing – review & editing, Supervision, Methodology, Formal analysis, Conceptualization.

Declaration of Competing Interest

The authors declare that they have no known competing financial interests or personal relationships that could have appeared to influence the work reported in this paper.

Acknowledgements

The authors acknowledge the support from ESA under the CCI-AWU (Climate Change Initiative Anthropogenic Water Use) precursor project (contract n. 4000142449/23/I-NB).

Data availability

Data will be made available on request.

References

Allen, R.G., Pereira, L.S., Raes, D., Smith, M., 1998. Crop evapotranspiration-Guidelines for computing crop water requirements. FAO Irrig. Drain. Pap. 56, D05109.

Brocca, L., Ciabatta, L., Massari, C., Moramarco, T., Hahn, S., Hasenauer, S., Kidd, R., Dorigo, W., Wagner, W., Levizzani, V., 2014. Soil as a natural rain gauge: Estimating global rainfall from satellite soil moisture data. J. Geophys. Res. Atmospheres 119 (9), 5128–5141. https://doi.org/10.1002/2014jd021489.

Brocca, L., Massari, C., Ciabatta, L., Moramarco, T., Penna, D., Zuecco, G., Pianezzola, L., Borga, M., Matgen, P., Martínez-Fernández, J., 2015. Rainfall estimation from in situ soil moisture observations at several sites in Europe: an evaluation of the SM2RAIN algorithm. J. Hydrol. Hydromech. 63 (3), 201–209. https://doi.org/10.1515/johh-2015-0016.

Brocca, L., Tarpanelli, A., Filippucci, P., Dorigo, W., Zaussinger, F., Gruber, A., Fernández-Prieto, D., 2018. How much water is used for irrigation? A new approach exploiting coarse resolution satellite soil moisture products. Int. J. Appl. Earth Obs. Geoinf. 73, 752–766. https://doi.org/10.1016/j.jag.2018.08.023.

Brombacher, J., Rezende de Oliveira Silva, I., Degen, J., Pelgrum, H., 2022. A novel evapotranspiration based irrigation quantification method using the hydrological similar pixels algorithm. Agr. Water Manag. 267, 107602. https://doi.org/10.1016/j.agwat.2022.107602.

Bwambale, E., Naangmenyele, Z., Iradukunda, P., Agboka, K.M., Houessou-Dossou, E.A., Akansake, D.A., Chikabvumbwa, S.R., 2022. Towards precision irrigation management: A review of GIS, remote sensing and emerging technologies. Cogent Eng. 9 (1), 2100573.

Chen, Y., Colloff, M.J., Lukasiewicz, A., Pittock, J., 2021. A trickle, not a flood: Environmental watering in the Murray-Darling Basin, Australia. Mar. Freshw. Res. 72 (5), 601–619.

Chiarelli, D.D., Passera, C., Rosa, L., Davis, K.F., D'Odorico, P., Rulli, M.C., 2020a. The green and blue crop water requirement WATNEEDS model and its global gridded outputs. Sci. Data 7 (1), 273. https://doi.org/10.1038/s41597-020-00612-0.

Chiarelli, D.D., Passera, C., Rosa, L., Davis, K.F., D'Odorico, P., Rulli, M.C., 2020b. Glob. Gridded Dataset CropSpecif. Green. Blue Water Requir. figshare. https://doi.org/10.6084/M9.FIGSHARE.C.4893084.V1.

Chiarelli, D.D., D'Odorico, P., Müller, M.F., Mueller, N.D., Davis, K.F., Dell'Angelo, J., Penny, G., Rulli, M.C., 2022. Competition for water induced by transnational land acquisitions for agriculture. Nat. Commun. 13 (1), 505. https://doi.org/10.1038/s41467-022-28077-2.

Dari, J., Brocca, L., Quintana-Seguí, P., Escorihuela, M.J., Stefan, V., Morbidelli, R., 2020. Exploiting High-Resolution Remote Sensing Soil Moisture to Estimate Irrigation Water Amounts over a Mediterranean Region. Remote Sens. 12 (16), 2593. https://doi.org/10.3390/rs12162593.

Dalezios, N.R., Dercas, N., Faraslis, I.N., Spiliotopoulos, M., Sidiropoulos, P., Sakellariou, S., Eslamian, S., 2023. Irrigation and Agrometeorology: Innovative Remote Sensing Applications in Crop Monitoring. In: Handbook of Irrigation Hydrology and Management. CRC Press, pp. 243–259. https://doi.org/10.1201/9780429290114-15.

Dari, J., Brocca, L., Modanesi, S., Massari, C., Tarpanelli, A., Barbetta, S., Quast, R., Vreugdenhil, M., Freeman, V., Barella-Ortiz, A., Quintana-Seguí, P., Bretreger, D., Volden, E., 2023. Regional data sets of high-resolution (1 and 6 km) irrigation estimates from space. Earth Syst. Sci. Data 15 (4), 1555–1575. https://doi.org/10.5194/essd-15-1555-2023.

Dari, J., Filippucci, P., Brocca, L., 2024. The development of an operational system for estimating irrigation water use reveals socio-political dynamics in Ukraine. Hydrol. Earth Syst. Sci. 28 (12), 2651–2659. https://doi.org/10.5194/hess-28-2651-2024.

Dari, J., Lo Presti, S., Brocca, L., 2025. Irrigation monitoring from satellite at hyper-high resolution: Paving the way for remote-sensing-based agricultural water management support services. Agric. Water Manag. 317, 109627. https://doi.org/10.1016/j.agwat.2025.109627.

Dari, Jacopo, Quintana-Seguí, Pere, Morbidelli, Renato, Saltalippi, Carla, Flammini, Alessia, Giugliarelli, Elena, Escorihuela, María José, Stefan, Vivien, Brocca, Luca, 2022. Irrigation estimates from space: Implementation of different approaches to model the evapotranspiration contribution within a soil-moisture-based inversion algorithm. Agric. Water Manag. https://doi.org/10.1016/j.agwat.2022.107537.

Devineni, N., Perveen, S., Lall, U., 2022. Solving groundwater depletion in India while achieving food security. Nat. Commun. 13 (1), 1–10. https://doi.org/10.1038/s41467-022-31122-9.

Eini, M.R., Massari, C., Piniewski, M., 2023. Satellite-based soil moisture enhances the reliability of agro-hydrological modeling in large transboundary river basins. Sci. Total Environ. 873, 162396. https://doi.org/10.1016/j.scitotenv.2023.162396.

Famiglietti, J.S., Lo, M., Ho, S.L., Bethune, J., Anderson, K.J., Syed, T.H., Swenson, S.C., De Linage, C.R., Rodell, M., 2011. Satellites measure recent rates of groundwater depletion in California's Central Valley. Geophys. Res. Lett. 38 (3), 2–5. https://doi.org/10.1029/2010GL046442.

FAO, 2024. FAOSTAT Statistical Database. Food and Agriculture Organization of the United Nations, Rome. Available at: ⟨https://www.fao.org/faostat⟩.

Foster, T., Mieno, T., Brozović, N., 2020. Satellite-Based Monitoring of Irrigation Water Use: Assessing Measurement Errors and Their Implications for Agricultural Water Management Policy. Water Resour. Res. 56.

Galli, N., Chiarelli, D.D., Ricciardi, L., Rulli, M.C., 2023. A Blue Water Scarcity-Based Method for Hydrologically Sustainable Agricultural Expansion Design. Water Resour. Res. 59 (10). https://doi.org/10.1029/2023WR034473.

Galli, N., Nanesha, H., Tolazzi, A., Chiarelli, D.D., Rulli, M.C., 2025. AIDA 1 km Resolut. Crop Specif. rainfed Irrig. Areas Green. blue Water Demands Italy 1–12.

Hersbach, H., Bell, B., Berrisford, P., Hirahara, S., Horányi, A., Muñoz-Sabater, J., Nicolas, J., Peubey, C., Radu, R., Schepers, D., Simmons, A., Soci, C., Abdalla, S., Abellan, X., Balsamo, G., Bechtold, P., Biavati, G., Bidlot, J., Bonavita, M., Thépaut, J., 2020. The ERA5 global reanalysis. Q. J. R. Meteorol. Soc. 146 (730), 1999–2049. https://doi.org/10.1002/qj.3803.

Hoogeveen, J., Faurès, J.M., Peiser, L., Burke, J., de Giesen, N.V., 2015. GlobWat–a global water balance model to assess water use in irrigated agriculture. Hydrol. Earth Sys. Sci. Discuss. 12, 3829–3844.

Huang, Z., Hejazi, M., Tang, Q., Vernon, C.R., Liu, Y., Chen, M., Calvin, K., 2019. Global agricultural green and blue water consumption under future climate and land use changes. J. Hydrol. 574, 242–256. https://doi.org/10.1016/j.jhydrol.2019.04.046.

Iglesias, A., Garrote, L., Flores, F., Moneo, M., 2007. Challenges to Manage the Risk of Water Scarcity and Climate Change in the Mediterranean. Water Resour. Manag. 21, 775–788. https://doi.org/10.1007/s11269-006-9111-6.

Jalilvand, E., et al., 2023. Is It Possible to Quantify Irrigation Water-Use by Assimilating a High-Resolution Satellite Soil Moisture Product? Water Resour. Res. 59.

Jalilvand, E., Tajrishy, M., Ghazi Zadeh Hashemi, S.A., Brocca, L., 2019. Quantification of irrigation water using remote sensing of soil moisture in a semi-arid region. Remote Sens. Environ. 231, 111226. https://doi.org/10.1016/j.rse.2019.111226.

Kebede, E., Oluoch, K.O., Siebert, S., Hartman, S., Mehta, P., Jägermeyr, J., Ray, D., Ali, T., Brauman, K.A., Deng, Q., Xie, W., Davis, K.F., 2024. A global open-source dataset of monthly irrigated and rainfed cropped areas (MIRCA-OS) for the 21st century. HydroShare 1–28. https://doi.org/10.1038/s41597-024-04313-w.

Kelly, T.D., Foster, T., 2021. AquaCrop-OSPy: Bridging the gap between research and practice in crop-water modeling. Agric. Water Manag. https://doi.org/10.1016/j.agwat.2021.106976.

Koch, J., Zhang, W., Martinsen, G., He, X., Stisen, S., 2020. Estimating net irrigation across the north China plain through dual modeling of evapotranspiration. Water Resour. Res. 56 (12). https://doi.org/10.1029/2020wr027413.

Kragh, S.J., et al., 2024. An inter-comparison of approaches and frameworks to quantify irrigation from satellite data. Hydrol. Earth Syst. Sci. 28, 441–457.

Kragh, S.J., Fensholt, R., Stisen, S., Koch, J., 2023. The precision of satellite-based net irrigation quantification in the Indus and Ganges basins. Hydrol. Earth Syst. Sci. 27, 2463–2478. https://doi.org/10.5194/hess-27-2463-2023.

Laluet, P., Dari, J., Busschaert, L., Heyvaert, Z., Brocca, L., Massari, C., Modanesi, S., Dorigo, W., Langhans, P., De Lannoy, G., Bechtold, M., Saltalippi, C., Morbidelli, R., Rulli, M.C., Chiarelli, D.D., Galli, N., 2025. Regional datasets of long-term and coarse resolution irrigation estimates from space [Data set]. Zenodo. https://doi.org/10.5281/zenodo.14988198.

Laluet, P., Dari, J., Busschaert, L., Heyvaert, Z., De Lannoy, G., Langhans, P., Modanesi, S., Massari, C., Brocca, L., Saltalippi, C., Morbidelli, R., Albergel, C., & Dorigo, W. (2026). Long-term irrigation water use datasets from multiple Earth Observation-based methods in major irrigated regions (Vol. 14988197, Issue January, pp. 1–30). https://doi.org/10.5194/essd-2025-737.

Lawston, P.M., Santanello Jr., J.A., Kumar, S.V., 2017. Irrigation signals detected from SMAP soil moisture retrievals. Geophys. Res. Lett. 44, 11–860. https://doi.org/10.1002/2017GL075733.

Lo, M.H., Famiglietti, J.S., 2013. Irrigation in California's Central Valley strengthens the southwestern U.S. water cycle. Geophys. Res. Lett. 40 (2), 301–306. https://doi.org/10.1002/grl.50108.

Maltby, E., 2006. River basin management and delta sustainability: A commentary on the Ebro Delta and the Spanish National Hydrological Plan. Ecol. Eng. https://doi.org/10.1016/J.ECOLENG.2005.01.005.

Martens, B., Miralles, D.G., Lievens, H., van der Schalie, R., de Jeu, R.A.M., Fernández-Prieto, D., Beck, H.E., Dorigo, W.A., Verhoest, N.E.C., 2017. GLEAM v3: satellite-based land evaporation and root-zone soil moisture. Geosci. Model Dev. 10 (5), 1903–1925. https://doi.org/10.5194/gmd-10-1903-2017.

Mehta, P., Siebert, S., Kummu, M., Deng, Q., Ali, T., Marston, L., Xie, W., Davis, K., 2022. Glob. Area Equipped Irrig. Dataset 19002015 (Version 2) [Dataset]. Zenodo. https://doi.org/10.5281/ZENODO.6886564.

Mehta, P., Siebert, S., Kummu, M., Deng, Q., Ali, T., Marston, L., Xie, W., Davis, K.F., 2024. Half of twenty-first century global irrigation expansion has been in water-stressed regions. Nat. Water 2 (3), 254–261. https://doi.org/10.1038/s44221-024-00206-9.

Mialyk, O., Booij, M.J., Schyns, J.F., Berger, M., 2024. Evolution of global water footprints of crop production in 1990-2019. Environ. Res. Lett. 19.

Nagaraj, D., Proust, E., Todeschini, A., Rulli, M.C., D'Odorico, P., 2021. A new dataset of global irrigation areas from 2001 to 2015. Adv. Water Resour. 152 (December 2020), 103910. https://doi.org/10.1016/j.advwatres.2021.103910.

Portmann, F., Siebert, S., Bauer, C., and Döll, P. (2008). Global data set of monthly growing areas of 26 irrigated crops, Version 1.0, Frankfurt Hydrol. Pap. 06, Inst. of Phys. Geogr., Univ. of Frankfurt, Frankfurt, Germany, 179–180 pp.

Puy, A., Sheikholeslami, R., Gupta, H.V., et al., 2022. The delusive accuracy of global irrigation water withdrawal estimates. Nat Commun 13, 3183. https://doi.org/10.1038/s41467-022-30731-8.

Rosa, L., Rulli, M.C., Davis, K.F., Chiarelli, D.D., Passera, C., D'Odorico, P., 2018. Closing the yield gap while ensuring water sustainability. Environ. Res. Lett. 13 (10), 104002. https://doi.org/10.1088/1748-9326/aadeef.

Siebert, S., Döll, P., 2008. The Global Crop Water Model (GCWM): Documentation and first results for irrigated crops. Frankfurt Hydrology Paper 07. Institute of Physical Geography, University of Frankfurt, Frankfurt am Main, Germany.

Siebert, S., Döll, P., 2010. Quantifying blue and green virtual water contents in global crop production as well as potential production losses without irrigation. J. Hydrol. 384 (3–4), 198–217. https://doi.org/10.1016/j.jhydrol.2009.07.031.

Tolomio, M., Casa, R., 2020. Dynamic crop models and remote sensing irrigation decision support systems: A review of water stress concepts for improved estimation of water requirements. Remote Sens. 12 (23), 3945.

Toureiro, C., Serralheiro, R., Shahidian, S., Sousa, A., 2017. Irrigation management with remote sensing: Evaluating irrigation requirement for maize under Mediterranean climate condition. Agric. Water Manag. 184, 211–220.

U.S. Department of Agriculture, Agricultural Research Service, Beltsville Human Nutrition Research Center. FoodData Central. [Internet]. [cited 26/11/2025]. Available from ⟨https://fdc.nal.usda.gov/⟩.

United States Drought Monitor (2022). Time series data. ⟨https://droughtmonitor.unl.edu/DmData/TimeSeries.aspx⟩.

Whitworth, K.L., Baldwin, D.S., Kerr, J.L., 2012. Drought, floods and water quality: Drivers of a severe hypoxic blackwater event in a major river system (the southern Murray-Darling Basin, Australia). J. Hydrol. 450–451, 190–198. https://doi.org/10.1016/j.jhydrol.2012.04.057.

Yao, Y., Thiery, W., Ducharne, A., Cook, B.I., Ding, A., De Hertog, S.J., Sieber, P., Aas, K. S., Arboleda-Obando, P.F., Colin, J., Costantini, M., Decharme, B., Lawrence, D.M., Lawrence, P., Leung, L.R., Lo, M.H., Devaraju, N., Wu, R.J., Zhou, T., Seneviratne, S. I., 2025. Irrigation-induced land water depletion aggravated by climate change. Nat. Water 3 (December). https://doi.org/10.1038/s44221-025-00529-1.

Zappa, L., Schlaffer, S., Brocca, L., Vreugdenhil, M., Nendel, C., Dorigo, W., 2022. How accurately can we retrieve irrigation timing and water amounts from (satellite) soil moisture? Int. J. Appl. Earth Obs. Geoinf. 113, 102979. https://doi.org/10.1016/j.jag.2022.102979.

Zappa, L., Dari, J., Modanesi, S., Quast, R., Brocca, L., De Lannoy, G., Massari, C., Quintana-Seguí, P., Barella-Ortiz, A., Dorigo, W., 2024. Benefits and pitfalls of irrigation timing and water amounts derived from satellite soil moisture. Agric. Water Manag. 295, 108773. https://doi.org/10.1016/j.agwat.2024.108773.

Zaussinger, F., Dorigo, W., Gruber, A., Tarpanelli, A., Filippucci, P., Brocca, L., 2019. Estimating irrigation water use over the contiguous United States by combining satellite and reanalysis soil moisture data. Hydrol. Earth Syst. Sci. 23 (2), 897–923. https://doi.org/10.5194/hess-23-897-2019.

Zhang, K., Li, X., Zheng, D., Zhang, L., Zhu, G., 2022. Estimation of Global Irrigation Water Use by the Integration of Multiple Satellite Observations. Water Resour. Res. 58, 1–23.

Zipper, S., Kastens, J., Foster, T., Wilson, B.B., Melton, F., Grinstead, A., Deines, J.M., Butler, J.J., Marston, L.T., 2024. Estimating irrigation water use from remotely sensed evapotranspiration data: accuracy and uncertainties at field, water right, and regional scales. Article 109036 doi Agric. Water Manag 303 (2024). https://doi.org/10.1016/j.agwat.2024.